Appl Phys B (2012) 106:893–898
DOI 10.1007/s00340-011-4758-y

Applied Physics B
Lasers and Optics

High-power passively Q-switched Nd:YVO_4 UV laser at 355 nm

Y.J. Huang · Y.P. Huang · P.Y. Chiang · H.C. Liang · K.W. Su · Y.-F. Chen

Received: 17 June 2011 / Revised version: 18 August 2011 / Published online: 11 October 2011

Abstract We report on an efficient high-power passively Q-switched UV laser at 355 nm. We take into account the second threshold criterion and the thermal-lensing effect to design and realize a compact reliable passively Q-switched Nd:YVO_4 laser with Cr^{4+}:YAG as a saturable absorber. At an incident pump power of 16.3 W, the average output power at 1064 nm reaches 6.2 W with a pulse width of 7 ns and a pulse repetition rate of 56 kHz. Employing the developed passively Q-switched laser to perform the extra-cavity harmonic generations, the maximum average output powers at 532 nm and 355 nm are up to 2.2 W and 1.62 W, respectively.

1 Introduction

In recent years, ultraviolet (UV) light sources have been rapidly developed because they are useful in many scientific research and industrial applications. Compared with other UV lasers, diode-pumped all-solid-state pulsed lasers with extra-cavity harmonic generations intrinsically possess advantages of smaller focused size, higher efficiency, longer life time, higher stability, easier implement and smaller system size etc. [1, 2]. Passively Q-switching of the solid-state laser with a saturable absorber can provide a reliable pulsed operation with the benefits of high stability, inherent compactness, and low cost. As a promising saturable absorber near the infrared region, Cr^{4+}:YAG crystal has been widely investigated on the passively Q-switched performance thanks to its good chemical and mechanical stability, long lifetime, excellent optical quality, high damage threshold, high thermal conductivity, and large absorption cross section [3–11].

Nd-doped vanadate crystals are characterized by their high absorption coefficients for diode pumping, large stimulated emission cross sections, and moderate thermal conductivities that are suitable for achieving excellent laser performance. Unfortunately, their stimulated emission cross sections at 1064 nm are too large to achieve the good passively Q-switched operations when the Cr^{4+}:YAG is used as a saturable absorber. Several methods have been proposed to overcome the second threshold of the passive Q-switching, including the intra-cavity focusing obtained from the three-element resonator [12–14] and the employment of a c-cut crystal as a gain medium [15–17]. However, the peak powers did not reach a critical level for efficient extra-cavity second and third harmonic generations (SHG and THG). As a result, high-power UV lasers at 355 nm based on passively Q-switched Nd:YVO_4/Cr^{4+}:YAG laser at 1064 nm have not been performed so far.

In this work, we design a high-peak-power passively Q-switched Nd:YVO_4 laser with Cr^{4+}:YAG as a saturable absorber for generating a high-power UV laser at 355 nm. We theoretically analyze and experimentally realize a compact passively Q-switched laser by considering the second threshold condition and the thermal-lensing effect. At an incident pump power of 16.3 W, the average output power reaches 6.2 W with a pulse width of 7 ns and a pulse repetition rate of 56 kHz. The corresponding pulse energy and peak power are found to be as high as 111 μJ and 16 kW, respectively. With the developed passively Q-switched laser to perform the extra-cavity SHG and THG, the maximum average output powers at 532 nm and 355 nm are found to

Y.J. Huang · Y.P. Huang · P.Y. Chiang · H.C. Liang · K.W. Su · Y.-F. Chen (✉)
Department of Electrophysics, National Chiao Tung University, 1001 TA Hsueh Road, Hsinchu, 30050 Taiwan
e-mail: yfchen@cc.nctu.edu.tw
Fax: +886-35-725230

be up to 2.2 W and 1.62 W, respectively. The optical-to-optical conversion efficiencies from 1064 nm to 355 nm and 808 nm to 355 nm are up to 26% and 10%, respectively. To our knowledge, this is the highest conversion efficiency for the 355-nm UV laser generated by the passively Q-switched Nd:YVO_4/Cr^{4+}:YAG laser.

2 Cavity analysis

It is well known that the absorption saturation in the saturable absorber should occur earlier than the gain saturation in the laser crystal for good passively Q-switched operation. The so-called second threshold condition has been analytically derived from the coupled rate equation, which can be mathematically expressed as [12, 18]

$$\frac{\ln(1/T_0^2)}{\ln(1/T_0^2)+\ln(1/R_{\mathrm{OC}})+L}\frac{\sigma_{\mathrm{gsa}}}{\sigma}\frac{A}{A_{\mathrm{s}}} > \frac{\gamma}{1-\beta}, \tag{1}$$

where T_0 is the initial transmission of the saturable absorber, R_{OC} is the reflectivity of the output coupler, L is the nonsaturable round-trip dissipative loss of the resonator, σ_{gsa} is the ground-state absorption of the saturable absorber, σ is the emission cross section of the laser crystal, A/A_{s} is the ratio of the laser mode area in the laser crystal to that in the saturable absorber, γ is the population inversion reduction factor, which is equals to one for the ideal four-level laser and two for the three-level laser, and $\beta = \sigma_{\mathrm{esa}}/\sigma_{\mathrm{gsa}}$ is the ratio of the excite excited-state absorption cross section to the ground-state absorption cross section of the saturable absorber. With the following parameters: $T_0 = 0.7$, $R = 0.5$, $L = 0.03$, $\sigma_{\mathrm{gsa}} = 2 \times 10^{-18}$ cm^2 [11], $\sigma = 25 \times 10^{-18}$ cm^2, $\gamma = 1$, and $\beta = 0.06$ [11], the second threshold condition can be deduced to be $A/A_{\mathrm{s}} > 2.68$ in the case of Nd:YVO_4 and Cr^{4+}:YAG as a gain medium and a saturable absorber, respectively. As a consequence, the ratio of the laser mode radius in the laser crystal to that in the saturable absorber needs to be larger than 1.64 for achieving a high-quality passively Q-switched operation.

The configuration for a simple plano-concave resonator with the thermal-lensing effect is schematically shown in Fig. 1(a). In the present experiment, the laser crystal and the saturable absorber are aimed to be as close as possible to the input concave mirror and the flat output coupler, respectively. An optical resonator with an internal thermal lens between the resonator mirrors can be replaced by an empty cavity with the equivalent g-parameters g^* and the equivalent cavity length L^*, which are given by [19]

$$g_i^* = g_i - \frac{1}{f_{\mathrm{th}}} d_j \left(1 - \frac{d_i}{R_i}\right), \tag{2}$$

$$g_i = 1 - \frac{d_1 + d_2}{R_i}, \tag{3}$$

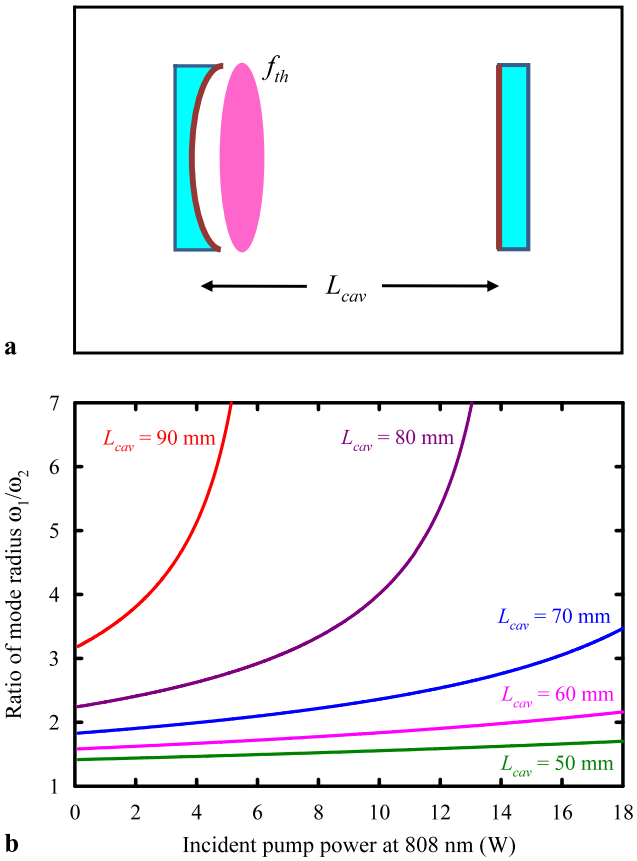

Fig. 1 (**a**) The configuration for a simple plano-concave cavity with the thermal-lensing effect; (**b**) calculated results for the ratio of the cavity mode size in the gain medium to that in the saturable absorber as a function of the incident pump power for the cases of $L_{\mathrm{cav}} = 90$ mm, 80 mm, 70 mm, 60 mm, and 50 mm when the radius-of-curvature of the input mirror is chosen to be $R = 100$ mm

$$i, j = 1, 2; \quad i \neq j,$$

$$L^* = d_1 + d_2 - \frac{1}{f_{\mathrm{th}}} d_1 d_2, \tag{4}$$

where f_{th} is the effective thermal focal length, d_1 and d_2 are the optical path length from the center of the gain medium to the input mirror and output coupler, R_1 and R_2 are the radius of curvature of the input mirror and output coupler. In terms of the equivalent cavity parameters, the cavity mode radius at the input mirror (ω_1) and at the output coupler (ω_2) are given by [19]

$$\omega_i = \sqrt{\frac{\lambda L^*}{\pi}\sqrt{\frac{g_j^*}{g_i^*(1 - g_1^* g_2^*)}}}, \quad i,\ j = 1, 2;\ i \neq j. \tag{5}$$

As a result, we can calculate the variations of the cavity mode radius ω_1 and ω_2 with respect to the effective thermal focal length. The effective focal length of thermal lens in the end-pumped laser crystal can be estimated with the

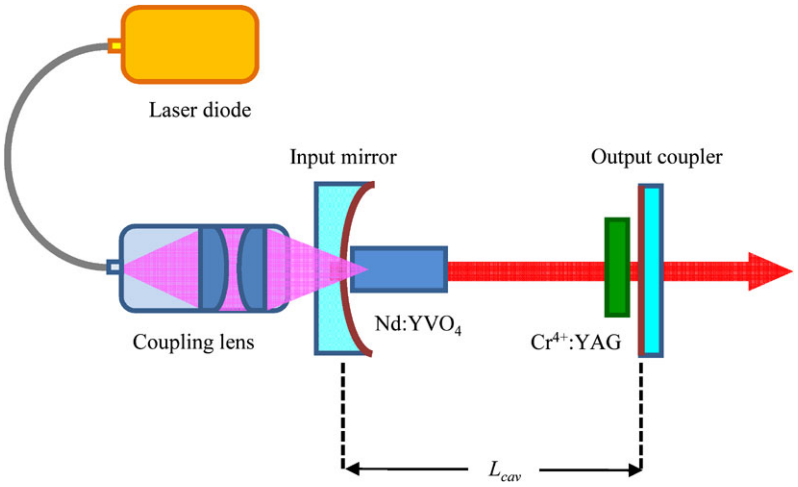

Fig. 2 Schematic of the cavity setup for a diode-pumped passively Q-switched Nd:YVO_4/Cr^{4+}:YAG laser

following equation [20]:

$$\frac{1}{f_{\text{th}}} = \frac{\xi P}{\pi K_c} \int_0^l \frac{\alpha e^{-\alpha z}}{1 - e^{-\alpha l}} \times \frac{1}{\omega_p^2(z)} \left[\frac{1}{2} \frac{dn}{dT} + (n-1)\alpha_T \frac{\omega_p(z)}{l} \right] dz, \tag{6}$$

where ξ is the fraction of the incident pump power that results in heat, P is the incident pump power, K_c is the thermal conductivity, α is the absorption coefficient, l is the crystal length, $\omega_p(z)$ is the variation of the pump radius, dn/dT is the thermal-optic coefficient, n is the refractive index, and α_T is the thermal expansion coefficient. With the following parameters: $\xi = 0.24$, $K_c = 5.23$ W/m K, $\alpha = 0.2$ mm^{-1}, $l = 12$ mm, $\omega_{po} = 300$ μm, $dn/dT = 3 \times 10^{-6}$ K^{-1}, $n = 2.1652$, and $\alpha_T = 4.43 \times 10^{-6}$ K^{-1}, the effective thermal focal length can be calculated as a function of the incident pump power. To be brief, the dependence of the ratio ω_1/ω_2 on the incident pump power can be generated to design and realize a high-quality passively Q-switched laser. Figure 1(b) depicts the calculated results for the cases of $L_{\text{cav}} = 90$ mm, 80 mm, 70 mm, 60 mm and 50 mm, where the L_{cav} stands for the cavity length and the other parameters used in calculation are as follows: $R_1 = 100$ mm, $R_2 \to \infty$, $d_1 = 6$ mm, $d_2 = (L_{\text{cav}} - 6)$ mm. From the Fig. 1(b), it is obvious that the thermal-lensing effect will make the cavity to be unstable when the cavity length is too long; whereas the passively Q-switched laser cannot well operate in a high-quality state when the cavity length is too short. Comparative speaking, we chose a resonator with $L_{\text{cav}} = 70$ mm to simultaneously satisfy the second threshold criterion and cavity-stability condition to realize a compact reliable passively Q-switched laser.

3 Experimental setup and results

The experimental setup is schematically shown in Fig. 2. The input mirror was a concave mirror with the radius-of-curvature of 100 mm. It was antireflection (AR) coated at 808 nm on the entrance face, and was coated at 808 nm for high transmission as well as 1064 nm for high reflection on the second surface. The gain medium was a 0.1 at.% a-cut Nd:YVO_4 crystal with dimensions of $3 \times 3 \times 12$ mm^3, and it was placed as close as possible to the input mirror. Both facets of the laser crystal were AR coated at 808 nm and 1064 nm. The Cr^{4+}:YAG saturable absorber with an initial transmission of 70% was AR coated at 1064 nm on both surfaces, and it was placed near to the output coupler. The laser crystal and the saturable absorber were wrapped with indium foils and mounted in water-cooled copper heat sinks at 20°C. The pump source was a 18-W 808-nm fiber-coupled laser diode with a core diameter of 600 μm and a numerical aperture of 0.2. The pump beam was re-imaged into the laser crystal with a lens set that has the focal length of 25 mm with a magnification of unity and the coupling efficiency of 91%. Therefore, the maximum incident pump power in our experiment is approximately 16.3 W. The flat output coupler with 50% transmission was employed during the experiment. As designed in Sect. 2, the cavity length was set to be 70 mm for the construction of the compact high-power passively Q-switched laser. The pulse temporal behaviors were recorded by a LeCroy digital oscilloscope (Wavepro 7100, 10 G samples/s, 1 GHz bandwidth) with a fast Si photodiode.

First of all, the continuous-wave operation without the saturable absorber is studied. The average output power as a function of the incident pump power is presented by the red curve in Fig. 3(a). The pump threshold and the slope efficiency are determined to be 2.1 W and 62%, respectively. At the maximum incident pump power of 16.3 W, the average output power of 8.8 W is obtained, corresponding to

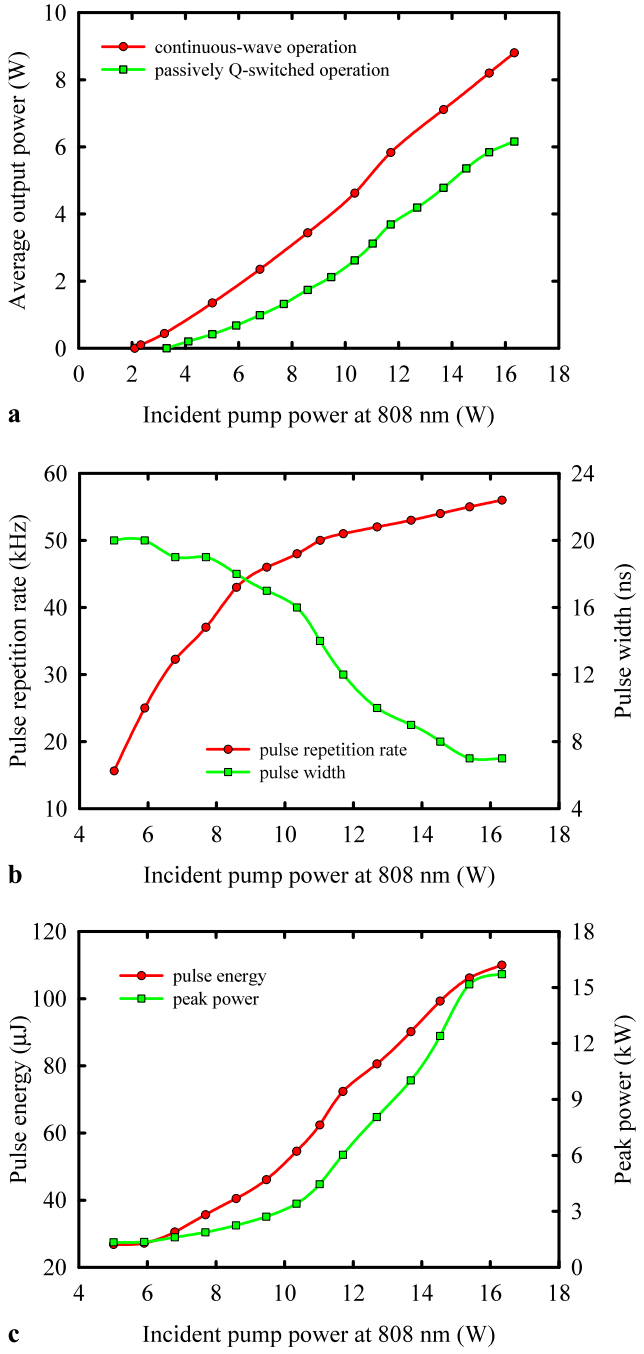

Fig. 3 (**a**) Average output powers in continuous-wave (*red curve*) and passively Q-switched (*green curve*) operations as a function of the incident pump power; (**b**) dependences of the pulse repetition rate (*red curve*) and pulse width (*green curve*) on the incident pump power; (**c**) dependences of the pulse energy (*red curve*) and peak power (*green curve*) on the incident pump power

the optical-to-optical conversion efficiency up to 54%. We then inserted the Cr^{4+}:YAG saturable absorber into the laser cavity to investigate the passively Q-switched performance in detail. The dependence of the average output power on the incident pump power in the passively Q-switched operation is illustrated by the green curve in Fig. 3(a). The pump threshold and the slope efficiency are found to be 3.3 W and 47.4%, respectively. At the maximum incident pump power of 16.3 W, the average output power as high as 6.16 W is obtained, corresponding to the optical-to-optical conversion efficiency up to 37.8%. Figures 3(b)–(c) show the pulse width, pulse repetition rate, pulse energy, and peak power as a function of the incident pump power. For the incident pump power increases from 5 W to 16.3 W, the pulse repetition rate varies from 15.5 kHz to 56 kHz and the pulse width changes from 20 ns to 7 ns, as shown in Fig. 3(b). Accordingly, it can be seen that the pulse energy increases from 27 μJ to 111 μJ and the peak power increases from 1.3 kW to 16 kW when the incident pump power increases from 5 W to 16.3 W, as revealed in Fig. 3(c). Note that the appearance of the satellite pulses following the main Q-switched pulse was frequently observed in the past research [21–24]. This phenomenon inevitably degrades the Q-switched performance, leading to the restriction of the maximum achievable Q-switched pulse energy and peak power. However, we did not observe any satellite pulses during the present experiment, indicating the validness of our cavity optimization. In the following section, we will employ this compact reliable high-power passively Q-switched laser to explore the performance in the processes of the extra-cavity SHG and THG.

4 Conversion efficiencies of extra-cavity harmonic generations

Here lithium triborate (LBO) crystals are exploited as nonlinear frequency converters for SHG and THG since they have the advantages of high damage threshold, relatively large acceptance angle, and small walk-off angle. One LBO crystal with dimensions of $3 \times 3 \times 15$ mm^3 was cut at $\theta = 90°, \phi = 10.4°$ for type-I phase-matched SHG at temperature of 46.6°C. Both facets of the SHG crystal were AR coated at 1064 nm and 532 nm. Another LBO crystal with dimensions of $3 \times 3 \times 10$ mm^3 was cut at $\theta = 44°, \phi = 90°$ for type-II phase-matched THG at temperature of 48°C. Both facets of the THG crystal were AR coated at 1064 nm, 532 nm, and 355 nm. The temperatures of the SHG and THG nonlinear crystals were monitored by thermoelectric controllers with the precision of 0.1°C. Two convex lenses were used to focus the laser beams into the SHG and THG nonlinear crystals for achieving efficient harmonic generations. The former one with focal length of 38 mm was AR coated at 1064 nm on both sides, the latter one with focal length of 19 mm was AR coated at 1064 nm and 532 nm on both sides. The optimized geometrical distances of L_1, L_2, L_3 and L_4 indicated in Fig. 4 were experimentally determined to be approximately 100 mm, 50 mm, 40 mm, and 20 mm,

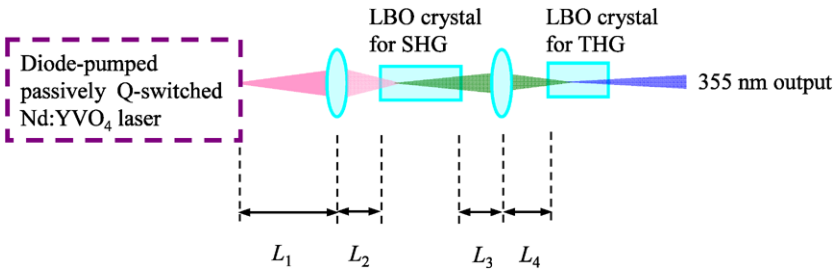

Fig. 4 Schematic of the experimental setup for the extra-cavity SHG and THG

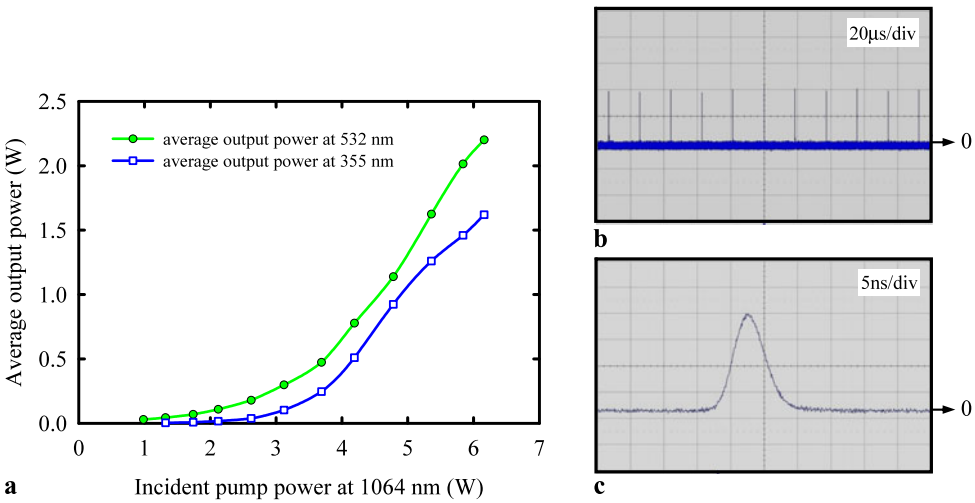

Fig. 5 (**a**) Dependences of the average output power at 532 nm (*green curve*) and 355 nm (*blue curve*) on the incident pump power at 1064 nm; typical temporal behaviors at 355 nm with: (**b**) time span of 200 μs, and (**c**) time span of 50 ns

respectively. The spot radii inside the SHG and THG nonlinear crystals were estimated to be about 71 μm and 38 μm, respectively.

The dependences of the average output powers at 532 nm and 355 nm on the incident pump power at 1064 nm are shown in Fig. 5(a). At the maximum incident pump power of 6.3 W at 1064 nm, the highest average output powers at 532 nm and 355 nm reach 2.2 W and 1.62 W with a pulse width as short as 5 ns and a pulse repetition rate of 56 kHz. Accordingly, the highest pulse energies at 532 nm and 355 nm are found to be 39 μJ and 29 μJ. More importantly, the largest peak powers at 532 nm and 355 nm as high as 7.8 kW and 5.8 kW are achieved. The optical-to-optical conversion efficiencies from 1064 to 355 nm and 808 nm to 355 nm are up to 26% and 10%, respectively. With a knife-edge method, the beam quality factors at 355 nm for orthogonal direction were measured to be $M_x^2 < 1.2$ and $M_y^2 < 1.3$, respectively. Typical temporal behaviors of the output pulses at 355 nm are shown in Figs. 5(b)–(c) with time span of 200 μs and 50 ns, respectively. The pulse-to-pulse amplitude fluctuation is found to be better than ±3%.

Finally, it is worthwhile to mention that although the intra-cavity focusing obtained from the three-element resonator can effectively enlarge the ratio of the laser mode area in the gain medium to that in the saturable absorber to meet the second threshold condition, it will not only add complexities to the overall laser cavity but also reduce the peak power that is detrimental for efficient extra-cavity harmonic generations. Employing a c-cut Nd:YVO_4 that has smaller stimulated emission cross section is another suitable way to satisfy the second threshold condition; however, the non-polarized laser output is problematic in the processes of harmonic generations, in which the linearly polarized fundamental beam is usually required. Comparative speaking, using a simple plano-concave resonator to construct a compact high-power passively Q-switched Nd:YVO_4/Cr^{4+}:YAG laser with constantly linear polarization is a practical method to simultaneously satisfy the second threshold condition and provide adequate peak power for efficient extra-cavity harmonic generations.

5 Conclusion

In summary, we have considered the second threshold criterion and the thermal-lensing effect to design a high-peak-power passively Q-switched Nd:YVO_4 laser with Cr^{4+}:YAG as a saturable absorber. At an incident pump power of 16.3 W, the average output power was found to reach 6.2 W with a pulse width of 7 ns and a pulse repetition rate of 56 kHz. The corresponding pulse energy and peak power were as high as 111 μJ and 16 kW, respectively. We further employed the developed passively Q-switched laser to perform the extra-cavity SHG and THG. At an incident pump power of 16.3 W, the average output powers

at 532 nm and 355 nm were found to be up to 2.2 W and 1.62 W, respectively. The optical-to-optical conversion efficiencies from 1064 nm to 355 nm and 808 nm to 355 nm were 26% and 10%, respectively. The excellent conversion efficiency in the generation of UV light confirms the theoretical analysis of the cavity design.

The authors thank the National Science Council for their financial support of this research under Contract No. NSC-97-2112-M-009-016-MY3.

References

1. A.V. Hicks, C.X. Wang, G.Y. Wang, Proc. SPIE **5332**, 120 (2004)
2. C.X. Wang, G.Y. Wang, A.V. Hicks, D.R. Dudley, H.Y. Pang, N. Hodgson, Proc. SPIE **6100**, 610019 (2006)
3. P. Yankov, J. Phys. D, Appl. Phys. **27**, 1118 (1994)
4. Y. Shimony, Y. Kalisky, B.H.T. Chai, Opt. Mater. **4**, 547 (1995)
5. Y. Shimony, Z. Burshtein, A.B.A. Baranga, Y. Kalisky, M. Strauss, IEEE J. Quantum Electron. **32**, 305 (1996)
6. T. Dascalu, G. Philipps, H. Weber, Opt. Laser Technol. **29**, 145 (1997)
7. X. Zhang, S. Zhao, Q. Wang, Q. Zhang, L. Sun, S. Zhang, IEEE J. Quantum Electron. **33**, 2286 (1997)
8. G. Xiao, J.H. Lim, S. Yang, E.V. Stryland, M. Bass, L. Weichman, IEEE J. Quantum Electron. **35**, 1086 (1999)
9. A. Suda, A. Kadoi, K. Nagasaka, H. Tashiro, K. Midorikawa, IEEE J. Quantum Electron. **35**, 1548 (1999)
10. A.G. Okhrimchuk, A.V. Shestakov, Phys. Rev. B **61**, 988 (2000)
11. A. Sennaroglu, U. Demirbas, S. Ozharar, F. Yaman, J. Opt. Soc. Am. B **23**, 241 (2006)
12. Y. Bai, N. Wu, J. Zhang, J. Li, S. Li, J. Xu, P. Deng, Appl. Opt. **36**, 2468 (1997)
13. C. Li, J. Song, D. Shen, N.S. Kim, J. Lu, K. Ueda, Appl. Phys. B **70**, 471 (2000)
14. C. Du, J. Liu, Z. Wang, G. Xu, X. Xu, K. Fu, X. Meng, Z. Shao, Opt. Laser Technol. **34**, 699 (2002)
15. Y.F. Chen, Y.P. Lan, Appl. Phys. B **74**, 415 (2002)
16. J. Liu, J. Yang, J. He, Opt. Commun. **219**, 317 (2003)
17. H. Yu, H. Zhang, Z. Wang, J. Wang, Z. Shao, M. Jiang, Opt. Express **15**, 3206 (2007)
18. Y.F. Chen, Y.P. Lan, H.L. Chang, IEEE J. Quantum Electron. **37**, 462 (2001)
19. N. Hodgson, H. Weber, *Laser Resonators and Beam Propagation*, 2nd edn. (Springer, Berlin, 2005), Chap. 8
20. W. Koechner, *Solid-State Laser Engineering*, 6th edn. (Springer, Berlin, 2005), Chap. 7
21. J. Bartschke, K.-J. Boller, R. Wallenstein, I.V. Klimov, V.B. Tsvetkov, I.A. Shcherbakov, J. Opt. Soc. Am. B **14**, 3452 (1997)
22. J. Liu, B. Ozygus, S. Yang, J. Erhard, U. Seelig, A. Ding, H. Weber, X. Meng, L. Zhu, L. Qin, C. Du, X. Xu, Z. Shao, J. Opt. Soc. Am. B **20**, 652 (2003)
23. S.P. Ng, D.Y. Tang, L.J. Qin, X.L. Meng, Opt. Commun. **229**, 331 (2004)
24. S.P. Ng, D.Y. Tang, L.J. Qian, L.J. Qin, IEEE J. Quantum Electron. **42**, 625 (2006)